Gaussian ensemble: An alternate Monte Carlo scheme

Murty S. S. Challa
Department of Physics and Astronomy and Center for Fundamental Materials Research, Michigan State University, East Lansing, Michigan 48824-1116

J. H. Hetherington
Department of Physics and Astronomy, Michigan State University, East Lansing, Michigan 48835-1116
(Received 24 June 1988)

The recently introduced Gaussian ensemble involves a sample (of size N) thermally connected to a *finite* heat bath (of size N') with specific properties. Treating N' as a parameter, we use a leading-order analysis of the β (inverse temperature) -versus-E (energy of sample) curves to show how static properties of finite samples become ensemble dependent. Inflection points in $\beta(E)$ at phase transitions, however, appear as nontrivial fixed points with respect to N' and are defined as the transition temperature of the sample. By developing a fluctuation relation for the heat capacity C we show that, for small N', states with $C<0$ are accessible at first-order transitions resulting in van der Waals loops in $\beta(E)$. Monte Carlo studies of phase transitions in Potts models on two- and three-dimensional lattices confirm the finite-N' and finite-N effects. We find that the method significantly reduces computer time (sometimes by a factor of 100) compared with canonical-ensemble simulations and is effective in diagnosing the order of phase transition. Specific-heat data at second-order transitions reveal a new phenomenon; the peak in C sharpens as N' becomes smaller, leading us to speculate on sharp transitions in finite samples.

I. INTRODUCTION

Statistical calculations of equilibrium properties of physical models involve closed systems consisting of a sample, whose properties we are seeking, in contact with a heat bath. If N and N' are the number of particles in the sample and heat bath, respectively, there are two broad classes of ensembles: those where N' is infinite (such as the canonical ensemble) and that where $N'=0$ (microcanonical ensemble). Computer simulations exploiting both classes of ensembles have been in vogue for over three decades now; well-known examples are the Monte Carlo method of Metropolis *et al.*,[1,2] using the canonical ensemble, and the molecular-dynamics method of Alder and Wainwright[3] and Rahman,[4] involving the microcanonical one.

It has been known for some time that systematic differences can arise between results using different simulation methods. The most dramatic of these occur at first-order transitions when we examine, for example, the temperature $1/\beta$ versus energy E curves. An isolated (i.e., microcanonical) system can go through a first-order phase transition by means of a succession of intermediate coexistence states, the only constraint being the constancy of E. If the system is finite, it will exhibit a negative specific heat due to interfacial tension (a simple argument is given for this in Sec. II) and van der Waals loops would show up if $\beta(E)$ is evaluated in the microcanonical ensemble (Fig. 1). It is known that such loops sometimes occur in molecular-dynamics simulations.[5,6] The coexistence states, however, have very low probability in the canonical ensemble so that energy distributions are double peaked and $\beta(E)$ simply possesses an inflection point like that at a continuous transition;[7,8] one then resorts to accurate extrapolations as $N\to\infty$ to diagnose the order of the transition.[7,9,10]

Since molecular dynamics is restricted to Hamiltonians where equations of motion can be constructed and is inapplicable to the stochastic models of order-disorder theory, there is a need for Monte Carlo methods which can approach the microcanonical limit. Apart from the obvious application to the study of phase diagrams, such techniques could lead to new insights into the nature of intermediate states at first-order transitions. Further, microcanonical Monte Carlo methods can provide independent verification of molecular-dynamics calculations. This would be useful, for example, in simulations of argon microclusters where the molecular-dynamics results of Jellinek *et al.*[11] show that the loops of Ref. 6 could be observed only during short runs and disappeared when long-time averages were taken.

A recent development in this respect was made by Creutz,[12] who considered a sample connected to a finite number of Ising ("demon") variables. Since the number of demons is a parameter, his method is an ensemble which interpolates between the microcanonical and canonical ensembles and one can approach the microcanonical limit in a controlled fashion. The only real problem with this method is that, except in some special cases, the entropy of the heat bath is an unknown function so that an extended analysis of the method is not possible. In particular, it is not possible to obtain a fluctuation result for the specific heat in Creutz's method.

The subject of this paper is the Gaussian ensemble,[13–17] which is a novel Monte Carlo technique introduced primarily to sample the coexistence states at first-

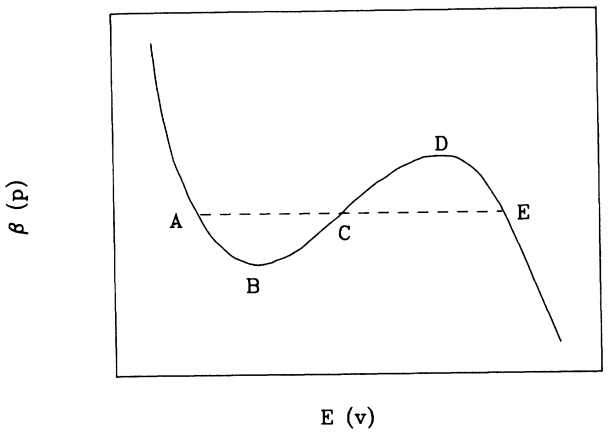

FIG. 1. Schematic diagram of a van der Waals loop in inverse temperature β vs energy E curves or pressure p vs volume v curves. The region of interest is BD and corresponds to states of negative specific heat and/or compressibility. AB and DE are described as regions of "superheating" and "supercooling" in an infinite sample. AE is Maxwell's equal-area construction. Note that we are referring to finite samples with finite-ranged interaction between the particles.

	SAMPLE	BATH
Number of particles	N	N'
Energy	E	E'
Entropy	S	$S' = -aE'^2$
Temperature	$T = 1/\beta$ $\beta = \partial S/\partial E$	$T' = 1/\beta'$ $\beta' = -2aE'$
Heat capacity	$C = -\beta^2/(\partial^2 S/\partial E^2)$	$C' = 2aE'^2$
	$E_t = E + E'$ $S_t = S + S'$	

FIG. 2. Closed system in the Gaussian ensemble showing the notation used. The sample and thermometer can exchange heat, and equilibrium is determined by $\beta=\beta'$. The ensemble is defined by the form of S' shown.

order transitions where it has been shown to produce the loops in $\beta(E)$. Operationally, the method consists of substituting the Boltzmann factor

$$e^{-\beta E}$$

in the canonical ensemble with the factor

$$\exp[-a(E-E_t)^2] ,$$

where a is a positive constant; the average temperature is then given by $\langle\beta\rangle=2a(\langle E\rangle-E_t)$. Thus the canonical ensemble, which imposes a definite temperature from which $\langle E\rangle$ is calculated, is replaced by a factor which specifies a linear combination of β and E. In brief, the theoretical basis of the method is as follows. Let S and E be the entropy and energy of the sample in the Gaussian ensemble and let primes denote the corresponding quantities of the "thermometer" (a small heat bath) (Fig. 2). All quantities are extensive unless otherwise stated. The total energy of the closed system is $E_t=E+E'$, the total entropy is $S_t(E)=S+S'$ and this ensemble is obtained[13] by specifying $S'=-a(E')^2=-a(E_t-E)^2$, where a is a positive constant. We adopt the view that the static properties of the sample are described uniquely by its density of states, $\rho(E)=\exp[S(E)]$, and that the thermometer is a tool for probing the derivatives of $S(E)$ by measuring the moments $\langle E\rangle$, $\langle E^2\rangle$, etc. This is equivalent to a microcanonical approach in that we characterize the sample by a set of energy levels and then derive the statistical properties from $\rho(E)$. To within an additive constant, the entropy is then defined, through $S(E)=\ln[\rho(E)]$ and β is obtained through $\beta=\partial S/\partial E$. (This is, in fact, the approach taken by some modern authors such as Reif,[18] Kittel,[19] and Pathria.[20]) Postulating equal *a priori* probabilities, the energy distribution is given by $P(E)\propto\rho(E)\rho'(E')\propto\exp[S_t(E)]$.

In this paper we present a comprehensive study which combines analysis and simulation to understand and validate the method. We find it fruitful to identify $a\propto 1/N'$ in the entropy of the bath and to use the method as an interpolating ensemble by assigning to a values from 0 to ∞.[17] By developing a fluctuation relation for the heat capacity C, we show that the loops are permitted for small N'. This ties in nicely with an explanation for the loops given by Alder and Wainwright,[5] who attributed them to the constraint on the density imposed in their molecular-dynamics simulations. (This has since been verified by Hansen and Verlet[21] and da Silva *et al.*[22] who have been able to obtain the loops in their canonical-ensemble Monte Carlo simulations by restraining the fluctuations.) The presence of the loops for small N' can indeed be interpreted in this fashion because the fluctuations vanish as $N'\to 0$. The merit of the Gaussian ensemble is that the fluctuations can be parametrized through N' in a continuous manner; a new result is we can show that for large (but *finite*) N' the loops disappear. There is another important benefit to viewing the method as an interpolating ensemble: we can thereby systematically account for N'-dependent effects in finite systems. It has always been appreciated, of course, that statistical averages of finite systems are ensemble dependent.[23,24] However, we find no evidence in the literature of any studies of these effects. Our analysis shows that, although $\langle\beta\rangle$, $\langle E\rangle$, etc. are ensemble independent for $N=\infty$, they are generally functions of N' for finite samples with the result that the averages obtained from the ensemble inevitably contain less information than the density of states itself. We present a convolution theorem on Gaussian integrals which also stresses the fundamental nature of $\rho(E)$ for finite samples: if the $\langle\beta\rangle$-versus-$\langle E\rangle$ curve is known for a given value of N', the corresponding curve for any *larger* value of N' can be predicted. Other things follow. It turns out that the N'-dependent deviations from the microcanonical values are prominent near phase transitions due to sizable fluctuations. However, inflection

points in $\beta(E)$ at phase transitions, denoted (β^*, E^*), are independent of N' to leading order in the energy fluctuations and thus constitute nontrivial fixed points with respect to N'. In this paper we shall use β^* as the transition temperature in a finite sample which will be extrapolated appropriately to obtain the infinite sample value.

We validate the analysis by comparing it with simulations of first- and second-order phase transitions in Potts models on "cubic" lattices in $d=2$ and 3 where d is the lattice dimensionality. Potts models are ideal for our purpose since many of their properties, such as the order of the transition are exactly known for $d=2$ and several approximate treatments of the models exist for $d=3$. Thus the emphasis is on the method and not on Potts models, although some of our results agree with the conjectures of other workers. We examine effects due to both finite N' and N and show that this is an effective method for diagnosing the order of a transition and would be very useful in investigating phase diagrams. We find that the sampling of the intermediate states drastically reduces the computer time at first-order transitions *vis-á-vis* canonical-ensemble simulations. Specific-heat data at second-order phase transitions reveal a novel phenomenon; although C is always found to be positive, the peaks in C for a given N sharpen remarkably as N' becomes smaller. This generates a discussion about sharp transitions in *finite* samples if the microcanonical ensemble were used to study the properties.

The rest of the paper is organized as follows. Section II is devoted to an analysis of the method. Section III deals with Potts models and the data from simulations. Section IV highlights the computational advantages of the method. Section V summarizes our findings and discusses future research.

II. ANALYSIS OF THE METHOD

A. Second-order Taylor's expansion of $S_t(E)$

We first demonstrate that the expression for the entropy of the bath, $S'=-a(E')^2$, is not as unphysical as it appears. Consider a bath of N' identical noninteracting classical Heisenberg spins in a magnetic field h. $\rho'(E')$ and hence, S', will be continuous functions because of the classical nature of the spins. If σ is the magnetic moment of each spin, the allowed values of E' are $-N'h\sigma \le E \le N'h\sigma$. At both these extreme values of E' the degeneracy of the energy level is 1 so that S' is 0 there and will therefore have a maximum at some $E'_{\max}$. Shifting the origin of both E' and S' to this point and expanding up to second-order, we obtain the form $S'=-a(E')^2$. Note that

$$a=\frac{1}{2}\left[\frac{\partial^2 S'}{\partial E'^2}\right]_{E'=0}>0$$

because S' has a maximum at the origin. Since these are noninteracting spins, both S' and E' are extensive and we can identify $a \propto 1/N'$. We shall sometimes refer to a instead of N' as a parameter.

For a given set of input parameters $\{a, E_t, N\}$ let the most probable energy for the sample be $\tilde{E}$ [i.e., where $S_t(\tilde{E})$ is a maximum]. Expanding $S_t(E)$ about $\tilde{E}$ we obtain, up to second order in small fluctuations of energy,

$$S_t(E)=S_t(\tilde{E})+\left[\frac{\partial S}{\partial E}+\frac{\partial S'}{\partial E}\right]_{E=\tilde{E}}(E-\tilde{E})$$
$$+\frac{1}{2}\left[\frac{\partial^2 S}{\partial E^2}+\frac{\partial^2 S'}{\partial E^2}\right]_{E=\tilde{E}}(E-\tilde{E})^2+\cdots . \quad (1)$$

We define the inverse temperature β and the heat capacity C through $\beta=\partial S/\partial E$ and $C=-\beta^2/(\partial^2 S/\partial E^2)$, thus extending the usual thermodynamic definitions to the case of finite N. The condition that S_t is a maximum, i.e., $(\partial S_t/\partial E)_{\tilde{E}}=0$, yields $\tilde{\beta}=\tilde{\beta}'$, which is the usual derivation of the equality of temperatures of systems in thermal equilibrium. Thus the second term in (1) vanishes and the probability of a sample of energy E,

$$P(E) \propto \exp[S_t(E)] ,$$

is a Gaussian centered on $\tilde{E}$ when only terms shown in (1) are retained. We obtain

$$\langle E \rangle = \tilde{E} , \quad (2a)$$

$$\langle \beta \rangle = \tilde{\beta} = 2a(\langle E \rangle - E_t) , \quad (2b)$$

and

$$\langle C \rangle = \tilde{C} = \frac{\tilde{\beta}^2 G_2}{1-2aG_2} , \quad (3)$$

where we have introduced the notation $G_n = \langle (E - \langle E \rangle)^2 \rangle$, $n=2,3,4,\ldots$. The tildes indicate that the quantities are the true (microcanonical) values and are to be evaluated at $\tilde{E}$.

We can verify that (3) is equivalent to $\langle C \rangle = -\langle \beta \rangle^2 \partial \langle E \rangle / \partial \langle \beta \rangle$ as follows. We define $Q_a(E_t)$, the analog of the partition function, through

$$Q_a = \sum_i \exp[-a(E_i - E_t)^2] , \quad (4)$$

where the subscript a denotes that we are considering a given bath. All quantities are now functions of E_t so that

$$\frac{\partial \ln Q_a}{\partial E_t} = \langle \beta \rangle = 2a(\langle E \rangle - E_t) , \quad (5)$$

$$\frac{\partial \langle E \rangle}{\partial E_t} = 2aG_2 , \quad (6)$$

and

$$\frac{\partial \langle \beta \rangle}{\partial E_t} = 2a(2aG_2 - 1) . \quad (7)$$

Using (6) and (7) in

$$\langle C \rangle = -\langle \beta \rangle^2 \left[\frac{\partial \langle E \rangle}{\partial E_t} \Big/ \frac{\partial \langle \beta \rangle}{\partial E_t}\right]$$

recovers (3). Note that Eq. (3) recovers the usual canonical-ensemble fluctuation formula for $\langle C \rangle$ in the

limit $a \to 0$. As another example of the interpolating properties of the ensemble, we see that $Q_a(E_t)$ reduces to the density of states $\rho(E) = \sum_i \delta(E - E_i)$ for $a \to \infty$, $E_t \to E$, and to the partition function $Z(\beta) = \sum_i \exp(-\beta E_i)$ in the limit $a \to 0$, $-2aE_t \to \beta$; thus the Gaussian ensemble interpolates smoothly between the two extremes.

Equation (3) also is a form of the fluctuation-dissipation theorem. The fluctuation G_2 can be written

$$G_2 \tilde{\beta}^2 = \tilde{C}\,\tilde{C}'/(\tilde{C} + \tilde{C}') ,$$

where C' is the heat capacity of the primed system. In our case where $S' = -a(E')^2$ we have

$$C' = \beta^2/2a .$$

This shows that for the purposes of the fluctuation theorem the heat capacities of the two systems in equilibrium add like capacitors in series.

A graphical interpretation of the method is given in Fig. 3. Define $S'' = -S' = a(E')^2$ or $S'' = a(E - E_t)^2$. For a given E_t, $\tilde{E}$ is then defined by the maximum in $S_t = S - S''$, i.e., the point where the slopes of S and S'' are equal. Since $\partial S''/\partial E$ is a single-valued function of E, we can evaluate β at any point on $S(E)$ by a proper choice of E_t. In the canonical limit, S'' is characterized only by its constant slope $\tilde{\beta}$ and coincides with the tangent. The probability of any state is then given by $P(E) \propto \exp(S - \tilde{\beta}E) \propto \exp(-\tilde{\beta}F)$ where $F = E - (S/\tilde{\beta})$ is the free energy of the state.

Figure 3 also explains the efficiency of the method. If a is large, the probability of the fluctuations away from $\tilde{E}$ falls off much more rapidly under this Gaussian sampling then under the canonical ensemble since $P(E) \propto \exp(S - S'')$. [This is also reflected in Eq. (3) where, if we keep $\tilde{\beta}$ and $\tilde{E}$ fixed, $G_2 \to 0$ as $a \to \infty$.] When a becomes very large, however, S'' becomes narrower, limiting the fluctuations, and considerably more computing time is necessary to achieve ergodicity.

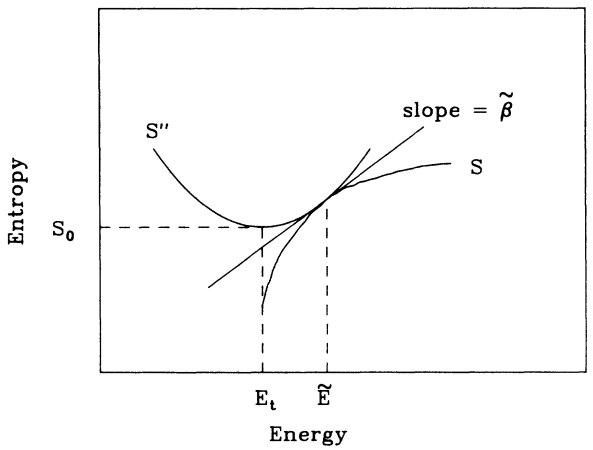

FIG. 3. Graphical interpretation of $\tilde{\beta}$ in the Gaussian ensemble. S is the entropy of the sample and $S'' = -S'$ where S' is the entropy of the bath. $\tilde{E}$, the most probable value of E, is the location of the maximum in $S_t = S - S''$. S'' has been shifted through a constant S_0 to make S and S'' touch at $\tilde{E}$. $\tilde{\beta}$ is the slope of the straight line and is simultaneously tangent to S and S''. $a \propto 1/N'$ is the curvature of S'' and the canonical ensemble is recovered when $a \to 0$, keeping $\tilde{\beta} = -2aE_t = \text{const}$; S'' then coincides with $\tilde{\beta}$.

B. Intermediate states at first-order transitions and negative specific heats

One is not completely unexposed to theories which look into the interphase region. Elementary texts contain p-V diagrams for the van der Waals equation of state. The isotherms are smooth functions which go through the interphase region and the transition pressure is to be calculated by an equal-area construction involving an integral over the interphase region. Nevertheless, most of us were taught not to attach any physical meaning to this region. Indeed, for several reasons the van der Waals theory is not very physical in that neighborhood. Mean-field theories (of which the van der Waals theory is an example) usually give loops in thermodynamic functions within the interphase region of a first-order transition[25] and these loops are an artifact of the mean-field approach. Nevertheless, one does not need to treat this region as taboo, since physically meaningful statements can be made.

Is it in fact possible to describe the interphase region in terms of equilibrium statistical mechanics? As shown in this section, it is certainly missed if "equilibrium" means "equilibrium with an infinite heat bath." On the other hand, real systems are often not in contact with an infinite heat bath but are more or less energetically isolated. For example, heat-capacity measurements are always made with the sample-calorimeter combination in equilibrium with each other but as isolated as possible as a whole. "Equilibrium" then means that the sample has the same temperature as the thermometer and that the sample is at a uniform temperature throughout. With this geometry there is no difficulty obtaining two coexistent phases in accord with ordinary experience, although as will be argued below, it is not possible for a pure substance when rigorous equilibrium with an infinite heat reservoir is maintained.

There are two very easily confused theorems implying that the second derivative of the entropy must be less than or equal to zero. If this is so, then temperature will rise or remain constant as energy is added to a system, that is, a system must have a positive heat capacity. Since we propose that negative heat capacities are possible, we must explore these theorems carefully.

Theorem 1. A sample in thermal equilibrium with an infinite heat bath will never be found to have an energy where $\partial^2 S/\partial E^2$ is positive.

Notice that the theorem does not say that S does not have positive curvature; just that it will never be found with an energy where that is true if it is in contact with a heat reservoir.

Sketch of proof. If two systems are in contact so that they share energy $E_t = E_1 + E_2$, then the probability of energy E_1 is

$$P(E_1) = P_1(E_1)P_2(E_t - E_1)$$

or

$$S_t(E_1)=S_1(E_1)+S_2(E_t-E_1)\ .$$

The most probable energy will be when $S_t(E_1)$ is a maximum, i.e., when

$$(\partial^2 S_t/\partial E_1^2)\leq 0$$

or

$$(\partial^2 S_1/\partial E_1^2)+(\partial^2 S_2/\partial E_2^2)\leq 0\ .$$

If system 2 is an *infinite reservoir,* then $\partial^2 S_2/\partial E_2^2=0$ and we require $\partial^2 S_1/\partial E_1^2\geq 0$ at the equilibrium energy $E_1=\bar{E}_1$. ■

Notice that only the *sum* of the second derivatives must be less than zero in the proof. In the case of the Gaussian ensemble this is equivalent to

$$2a+\frac{\beta^2}{C}\geq 0\ . \tag{8}$$

We see immediately that for N finite and $\tilde{C}<0$ we can find a large enough to stabilize the system. Thus the loops are permitted for small N'. In the limit of an infinite bath, however, $a=0$ so that $\beta^2/C\geq 0$ is required and we have theorem 1.

Theorem 2. A system consisting of an infinite but isolated pure substance will never have the second derivative of entropy positive because it could always break up into two phases such that the sum of the entropies is larger.

Sketch of proof. This can be derived by the following construction. Suppose to the contrary that $S(E)$ is positively curved as shown in Fig. 4. Consider two energies which are the extremes of a line which forms the convex hull of the curve $S(E)$, shown in Fig. 4 as E_A and E_B.

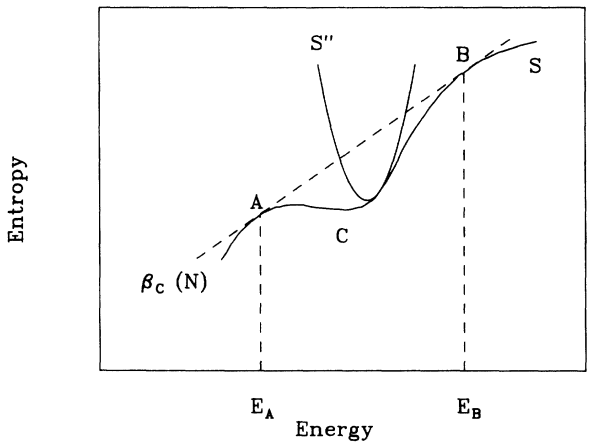

FIG. 4. Schematic diagram of the entropy at a first-order transition. The notation is that of Fig. 3. The *ACB* portion of the curve in S is due to the interface effects in a finite sample. $\beta_c(N)$ is the slope of the dashed line *AB* which denotes the entropy of an infinite heat bath. $\beta_c(N)$ is defined as the transition temperature of the sample if the canonical ensemble were used because of the equality of the free energies at this temperature. As the size of the sample increases, *ACB* approaches the line $\beta_c(N)$. The curve S'' shows that it is possible to sample the states near C using large a in the Gaussian ensemble.

Because the energy and the entropy are extensive (and implied by this is the fact that the surface energies and entropies are negligible) it is possible to re-form the system out of two phases of energy per particle E_A/N and E_B/N. The total entropy will be given by a similar combination of the entropies S_A and S_B:

$$S(E)=N_A(S_A/N)+N_B(S_B/N)$$
$$=[S_A(E_B-E)+S_B(E-E_A)]/(E_B-E_A)\ .$$

But this is just the equation for the straight line *AB* in Fig. 4. Thus in the infinite sample limit the S/N curve versus E/N curve will be convex, always curving downward or having zero curvature. ■

As hinted in the proof, however, the entropy of a finite system may be slightly below the convex hull derived for an infinite system because of the interface between the phases. Although the part of the entropy which goes like N is maximized by splitting the system into two phases, there are additional terms which go like the number of atoms in the interphase surface (that is, proportional to $N^{(d-1)/d}$). The effect on the entropy is negative or the surface area would maximize and the two phases would become one foglike phase. (And indeed, the effect on the entropy would be proportional to N because the surface area would increase until all the atoms were involved. This is, in fact, what happens in a one-dimensional system where the surface entropy is positive, thus prohibiting phase transitions.) We know therefore that because of this surface entropy, the total entropy of a two-phase system will lie slightly below the straight line implied by the derivation above. The size of the surface effect will be proportional to the area of the surface, which will depend in turn on the system energy because the amount of each phase is to first order just given by the argument above. Since this surface entropy effect is negative, it has the effect of causing an upward curvature when added to the linear two-phase line of theorem 2.

The existence of states with $C<0$ can also be understood through free-energy concepts using the following oversimplified argument. Consider the situation depicted in Fig. 5, where we have a sample on the verge of a first-order transition, and a small amount of the high-temperature phase nucleates upon adding some heat $\Delta Q=\Delta E$. Using the notation in the figure, the change in the free energy of the sample is $\Delta F=F'-F=N_s(f_s-f_-)$ where f_s is the surface free energy per particle and is proportional to the surface tension. Now $f_s>f_-$ or else the sample would have spontaneously broken up into a foglike phase by maximizing the area of the drops. An observer for whom the sample is a black box and who wishes to use thermodynamics will find that $\Delta F/\Delta E=-S/C>0$ so that he will conclude that $C<0$. At a second-order transition, on the other hand, the surface tension vanishes so that $C>0$. For infinite systems, N_s is negligible compared to N_+ and N_- so that $F'\approx N_+f_++N_-f_-$. But $f_+=f_-$ so $\Delta F=0$, resulting in an infinite specific heat (latent heat). This δ-function singularity in specific heat has also been verified through simulations.[7]

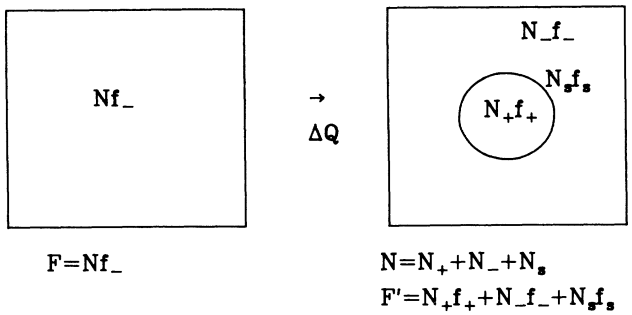

FIG. 5. Schematic diagram of nucleation at a first-order transition. The subscripts $-$ and $+$ refer to the low- and high-temperature phases, respectively, and the subscript s refers to surface quantities. f denotes free energy per particle. N is the total number of particles in the sample. F and F' are the total free energies before and after receiving the heat ΔQ. See text for discussion.

C. N' dependencies in $\langle E \rangle$ and $\langle \beta \rangle$

Equations (2), which result from a Gaussian approximation to $P(E)$, are good when the sample is far from a phase transition. However, the third-order term in (1) becomes appreciable at phase transitions due to the large fluctuations and we consider its effects approximately as follows. Define

$$\tilde{S}_3=\frac{1}{3!}\left[\frac{\partial^3 S}{\partial E^3}\right]_{E=\tilde{E}}, \quad \tilde{\sigma}^2=\frac{\tilde{C}}{2a\tilde{C}+\tilde{\beta}^2}, \quad z=3\tilde{S}_3\tilde{\sigma}^4 .$$

Now approximate $\exp[\tilde{S}_3(E-\tilde{E})^3]\approx 1+\tilde{S}_3(E-\tilde{E})^3$ in $P(E)$. This retains the Gaussian form of $P(E)$ and we obtain readily

$$\langle E \rangle=\tilde{E}+z , \tag{9a}$$

$$\langle E^2 \rangle=\tilde{E}^2+\tilde{\sigma}^2+2\tilde{E}z , \tag{9b}$$

and

$$\langle E^3 \rangle=\tilde{E}^3+3\tilde{E}^2 z+3\tilde{E}\tilde{\sigma}^2+5\tilde{\sigma}^2 z . \tag{9c}$$

Solving (9) for z yields

$$z^3+z(G_2/2)-(G_3/4)=0 . \tag{10}$$

The discriminant of (10), Δ, is given by $\Delta=(-G_3/4)^2+4(G_2/6)^3>0$ and yields only one real root for z. Specifically, if u^3 and v^3 are roots of $t^2+(-G_3/4)t-(G_2/6)^3=0$, then $z=u+v$, i.e.,

$$z=\frac{[(G_3/4)+\sqrt{\Delta}]^{1/3}}{2}+\frac{[(G_3/4)-\sqrt{\Delta}]^{1/3}}{2} . \tag{11}$$

Note that G_2 and G_3 are "measurable" quantities so that z can be estimated from simulations. We may express the temperature deviations as

$$\langle \beta \rangle=\tilde{\beta}+2az . \tag{12}$$

Equations (9a) and (12) then show that z is a measure of the deviations of $\langle E \rangle$ and $\langle \beta \rangle$ from the true values.

We may write

$$z=\frac{1}{2}\frac{\tilde{C}^2}{(\tilde{\beta}^2+2a\tilde{C})^2}\left[\frac{\partial^2\beta}{\partial E^2}\right]_{E=\tilde{E}} ,$$

where $\tilde{C}$ is of order N and $\partial^2\beta/\partial E^2$ is order N^{-2}. In the limit $a\to 0$, z is of order unity with the result that $\langle E \rangle/N\to(\tilde{E}/N)+O(1/N)$ and $\langle \beta \rangle\to\langle \tilde{\beta} \rangle$; this is, of course, the canonical result. Since $z\to 0$ in the microcanonical limit, we find that the true values are obtained for $a\to\infty$. Finite-N effects in the Gaussian ensemble are investigated by treating N as a parameter while maintaining $\lambda=N/N'\propto aN=$const. Then, $a\to 0$ as $N\to\infty$ so that $\langle E \rangle/N\to\tilde{E}/N$ and $\langle \tilde{\beta} \rangle\to\tilde{\beta}$. But this result is independent of the value of λ, showing that statistical averages of properties of macroscopic systems are independent of the ensemble used.

One of the useful features of Eq. (10) is that $G_3=0$ implies $z=0$ and vice versa. But

$$z\propto\left[\frac{\partial^2\beta}{\partial E^2}\right]_{E=\tilde{E}}$$

and hence inflection points in $\tilde{\beta}(\tilde{E})$ are independent of N'. The curves of $\langle \beta \rangle$ versus $\langle E \rangle$ for various a cross at these points, denoted by (β^*,E^*), which are thus nontrivial fixed points with respect to N'. $\beta=0$ and ∞ then represent trivial fixed points since $P(E)$ approaches a δ function at these extreme ($G_3\to 0$). In this paper we take β^* as an alternate choice for the transition temperature even at first-order transitions where it is an alternative to the equal-area construction. (We noticed significant a dependencies in β^* only at highly asymmetric first-order transitions; the equal-area[13] construction then provides a better definition of the transition temperature.)

Equations (9a) and (12) also allow a form of scaling. From $\langle \beta \rangle$ versus $\langle E \rangle$ for a given a we can estimate $\tilde{E}$ and $\tilde{\beta}$ and thus all the curves for various a (N fixed) should collapse onto a single curve, the microcanonical one. Of course, in view of the approximations made in obtaining these equations, we expect the results to be good only for large values of a (small fluctuations). This is confirmed by the simulation results which will be shown in Sec. III.

The preceding arguments show that, for finite, nonzero N and N', information is inevitably lost during statistical averaging. [By complete information we mean a knowledge of $\tilde{\beta}(\tilde{E})$.] This fact is also illustrated by the following theorem.

Theorem 3. Let $\beta_a(E_t)$ denote the curve $\langle \beta \rangle$ versus $\langle E \rangle$ for a given a. Then if we know $\beta_a(E_t)$, we can find $\beta_{a'}(E_t)$ for any other $a'<a$.

Proof. Rewrite (4) as

$$Q_a(E_t)=\int_{-\infty}^{+\infty}\rho(E)\exp[-a(E-E_t)^2]dE . \tag{13}$$

Then

$$\beta_a(E_t)=\frac{\partial \ln Q_a(E_t)}{\partial E_t} , \tag{14}$$

and we can write

$$Q_a(E_t)=\exp\left[\int^{E_t}\beta_a(E_t')dE_t'\right] . \tag{15}$$

Consider the integral

$$I=\int_{-\infty}^{+\infty}\exp[-b(E_t-E_t')^2]Q_a(E_t')dE_t' , \tag{16}$$

which becomes, by (13),

$$I=\int_{-\infty}^{+\infty}\rho(E)dE\int_{-\infty}^{+\infty}dE_t'\exp\{-[b(E_t-E_t')^2 +a(E-E_t')^2]\}$$

$$=(\pi/a+b)^{1/2}\int_{-\infty}^{+\infty}\rho(E)\exp\left[\frac{-ab}{a+b}(E-E_t)^2\right]dE . \tag{17}$$

Defining $a'=ab/(a+b)$, the integral is simply $Q_{a'}(E_t)$ so that (16) and (17) may be combined into

$$Q_{a'}(E_t)=[a^2/\pi(a-a')]^{1/2} \times\int_{-\infty}^{+\infty}\exp\left[\frac{-aa'}{(a-a')}(E_t-E_t')^2\right]Q_a(E_t') \times dE_t' . \tag{18}$$

$Q_a(E_t')$ can be numerically evaluated through (15) and thus $\beta_{a'}(E_t)$ can be predicted using (14) and (18). Apart from requirements of convergence of integrals, we need that $a>a'$ in order that $Q_{a'}(E_t)$ be a real quantity. ■

Therefore it is not possible to reconstruct the density of states of a finite system using canonical-ensemble averages, while it is always possible to obtain the canonical-ensemble averages from the Gaussian-ensemble averages through

$$Z(\beta)=(a/\pi)^{1/2}e^{-\beta^2/4a}\int Q_a(E)e^{-\beta E}dE .$$

III. SIMULATIONS

A. Potts models

We illustrate the validity of the method by simulating q-state Potts models[26] on square and simple-cubic lattices of side L with periodic boundary conditions ($N=L^d$). In a q-state Potts model the spin at the ith site, σ_i, can take one of q different values, say the numbers 1–q. The ferromagnetic Hamiltonian used in our simulations is given by

$$H=-J\sum_{(i,j)}\delta_{\sigma_i\sigma_j}-h\sum_i\delta_{\sigma_i 1} , \tag{19}$$

where δ is the Kronecker δ function. The first term in (19) is a sum over all the nearest-neighbor pairs with J (>0) being the interaction strength. The second term is the interaction of the spins with a field, h, which couples only to spins with $\sigma=1$. We shall mainly be concerned with models where $h=0$. We shall use units where energy is in units of J, β is in units of J^{-1}, and h is in units of J. The following notation is used. $\beta_c(\infty)$ is the inverse of the infinite-lattice transition temperature. Energies *per site* at the transitions in the infinite lattice are denoted by $E_c(\infty)$ if the transition is second order and by E_- and E_+ if the transition is first order. The notation $\beta^*(L)$ emphasizes the L dependence of β^*.

The advantage of Potts models is that the nature of the transition is q dependent: for $q\le q_c$ the transition is second order, while for $q>q_c$ the transition is first order. For $d=2$ and $h=0$, Baxter[27] has shown that $q_c=4$. Baxter's results for the transition temperature and the latent heat are

$$\beta_c(\infty)=\ln(1+\sqrt{q}) \tag{20}$$

and

$$E_+-E_-=2\left[1+\frac{1}{\sqrt{q}}\right]\tanh(\theta/2)\prod_{n=1}^{\infty}[\tanh(n\theta)]^2 , \tag{21}$$

where $2\cosh\theta=\sqrt{q}$. We can obtain E_+ and E_- separately by combining the above with the result of Kihara *et al.*:[28]

$$E_++E_-=-2(1+1/\sqrt{q}) . \tag{22}$$

The situation is not exactly known for $d=3$, $h=0$, although approximate calculations[26] suggest that $q_c=2$.

Monte Carlo realization of the Gaussian ensemble is straightforward. Phase space is sampled by going to each spin on the lattice in turn and then testing it for "flipping" from a configuration $\{\mu\}$ to a new configuration $\{\nu\}$. If P_μ and P_ν are the probabilities for two configurations of energies E_μ and E_ν, their relative probability is given by

$$\frac{P_\nu}{P_\mu}=\frac{\exp[-a(E_\nu-E_t)^2]}{\exp[-a(E_\mu-E_t)^2]} , \tag{23}$$

and the process is implemented on the computer by comparing the ratio to a random number as usual.[2] One pass over all the spins in the lattice constitutes a Monte Carlo step per site (MCS), and is taken as the unit of computer time. An important difference from canonical-ensemble Monte Carlo is that E_ν, E_μ are now the total energies of the lattice and not just the energies of the particular spin in question. In Appendix A we describe how to choose a and E_t conveniently when using the method for the first time.

B. Simulations of first-order transitions

Figures 6–9 deal with data from simulations of the $d=2$, $q=10$, $h=0$ model which has a strong first-order transition. Figure 6(a) shows the $\langle\beta\rangle$-versus-$\langle E\rangle$ curves for various a for $L=8$ and we see that the loops appear for large a (>0.001). The disappearance of the loops for small a coincides with the appearance of double-peaked energy distributions where the specific heat corresponding to the two peaks is positive; this has been explicitly shown in Ref. 17. The horizontal dashed line in this figure is the equal-area construction[13] and this agrees with the value of β^* obtained from the fixed-point concept. The curves in Fig. 6(a) are predictions based on the data for $a=0.05$ (not shown) and using theorem 3 of Sec. II C; the good agreement with the data supports the analysis. Figure 6(b) presents the specific-heat data ob-

tained from Eq. (3) for the curves in Fig. 6(a) and confirms the negative values for large a. Note that we have plotted $\langle E \rangle$ as the ordinate since $\langle C \rangle$ is a multivalued function of $\langle \beta \rangle$.

Figures 7(a)–7(c) pertain to the analysis of the third-order terms in $S_t(E)$ discussed in Sec. II C. Figures 7(a) and 7(b) show the behavior of G_3 and z, respectively, for various a and confirm that they vanish near E^* and also at the extreme values of the energy. Thus they validate the qualitative features of our analysis. The analysis is quantitatively tested by the scaling plot of Fig. 7(c),

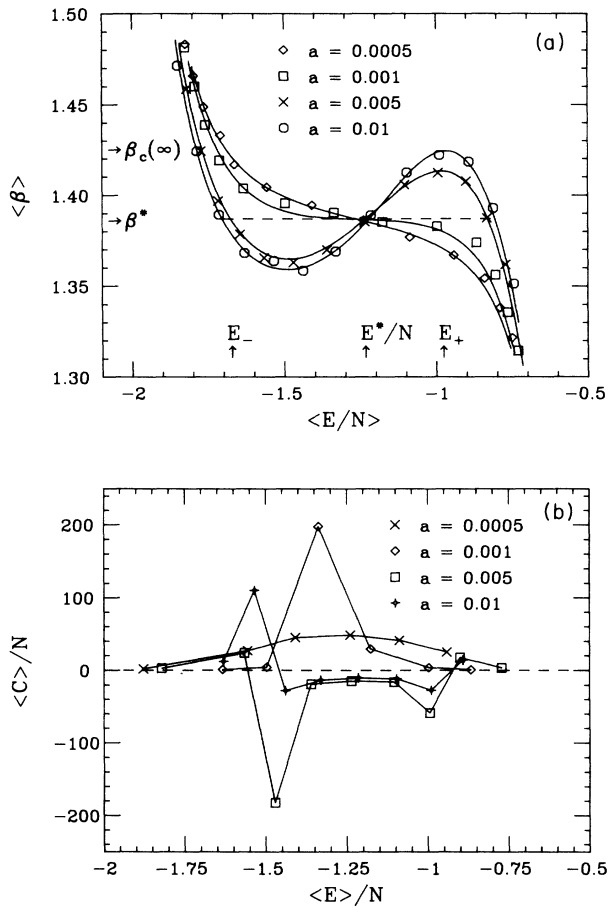

FIG. 6. (a) Typical $\langle \beta \rangle$-vs-$\langle E \rangle/N$ curves for $N=64$ and various a at a first-order transition. The symbols are Monte Carlo data for the $q=10$, $h=0$ model on an 8×8 lattice and are averages over 200 000 MCS each. The curves are predictions based on the data for $a=0.05$ (not shown) and using Eqs. (14) and (18). The loops are clearly seen as the microcanonical (large-a) limit is approached. The horizontal dashed line is the equal-area construction for $a=0.01$. (E^*,β^*) is the fixed point. $\beta_c(\infty)$, E_-, and E_+ are the infinite-lattice characteristics at the transition. (b) Specific heat as a function of energy at the first-order transition of (a). $\langle C \rangle$ is obtained from Eq. (3). $\langle C \rangle$ data for $a=0.001$ have been divided by 15 to include all the data in the figure. The horizontal dashed line represents $\langle C \rangle = 0$. Some data have been omitted for clarity. The curves are straight-line interpolations between data points. The loops in (a) for $a=0.005$ and 0.01 give rise to regions with $\langle C \rangle < 0$ here.

where we have plotted $\tilde{E}$ and $\tilde{\beta}$ obtained from Eqs. (9a) and (12). Although data for $a=0.05$, 0.01, and 0.005 fall on a single curve, the microcanonical one, significant deviations are seen for $a=0.001$ and 0.0005. This illustrates that the analysis is valid only for small fluctuations (large a).

Figures 8 and 9 present the finite-N effects at the above first-order transition which were investigated keeping the ratio $N/N' \propto aN = \text{const}$. As shown in Sec. II C, the properties of macroscopic samples are independent of N' so that we expect the loops to flatten out to a horizontal straight line as $N \to \infty$. This indeed happens in Fig. 8. Using $L=8$, 10, 12, 14, and 20 we determined $\beta^*(L)$ as in Fig. 6(a). Figure 9 shows the extrapolation of $\beta^*(L)$ versus L^{-d} in the manner of Ref. 7 to obtain $\beta_c(\infty)$. As is evident, the fit is very good and our value of $\beta_c(\infty)$ agrees well with the exact result.

C. Simulations of second-order transitions

Figures 10–12 deal with the second-order transition in the $d=2$, $q=3$, $h=0$ model. It has been shown in Ref. 17 that no loops are seen in $\langle \beta \rangle$ versus $\langle E \rangle$ at this transition and thus the method provides a clear distinction between first- and second-order transitions. The scaled data are shown in Fig. 10 and we once again see that the data collapse onto the microcanonical curve for large a. The data for G_3 and z are similar to those at first-order transitions [Figs. 7(a) and 7(b)] and thus are not presented here.

$\beta^*(L)$ was found in this fashion for $L=8$, 10, 12, 20, 22, and 26 and $\beta_c(\infty)$ was found by extrapolating $\beta^*(L)$ versus $L^{-1/\nu}$ in Fig. 11 using $\nu=\frac{5}{6}$ in keeping with den Nijs's conjecture[29] for $q=3$. (ν is the critical exponent for the correlation length ξ; thus $\xi \sim [\beta_c(\infty)-\beta]^{-\nu}$. See Ref. 9 for a discussion of the finite-size effects).

The specific-heat data pertaining to Fig. 10 are plotted in Fig. 12 and show remarkable N'-dependent effects. As a increases, we find that the peak in $\langle C \rangle/N$ grows and simultaneously sharpens, giving the impression of a cusp in the specific heat for large a. By verying that there were no significant changes in the data for $a>0.05$, we ruled out the possibility of a diverging specific heat. To confirm that the sharpening of $\langle C \rangle$ is linked to critical behavior, we also studied the ferromagnetic Ising model ($q=2$) in $d=3$ and the paramagnetic Ising model in a magnetic field. The results are presented in Figs. 13 and indeed, while the second-order transition in the $d=3$ Ising model does give rise to the "cusp," no such behavior is seen in the (noncritical) paramagnetic model.

Note that the arguments of Yang and Lee[30] prohibiting phase transitions in a finite sample are based on the (grand) canonical ensemble whereby the partition function is required to be analytic for finite N. [Indeed, Figs. 12 and 13(a) show correctly that any singularity is smeared out as the canonical ensemble is approached.] The same arguments hold for the Gaussian ensemble (for finite a) since

$$Q_a(E_t) = \sum_i \exp[-a(E_i - E_t)^2]$$

is an analytic function of E_t in the entire complex plane and is nonzero and positive for E_t on the real axis.

Therefore (5) shows that β is analytic as well for real E_t. However, $\beta(E_t)$ determined from the Gaussian ensemble can be much less smooth than that from the canonical ensemble because, as shown in Sec. II C, the canonical results can be obtained by smoothing the Gaussian results. In the limit $a \to \infty$, $Q_a(E_t)$ approaches $\rho(E)$ and the results are quite singular since $\rho(E)$ is a series of δ functions for any finite sample. The interesting question is whether one can give mathematical justification for the concept of a sharp phase transition in a finite sample even though the limit $a \to \infty$ is very irregular while a finite is technically analytic. There are other difficult questions when the notion of sharp transitions in finite samples is introduced. Thus we may ask: is there a lower bound on N such that for smaller samples there does not exist a sharp transition? If not, are there sharp transitions for, say, $N=2$? What is the meaning of β for such small samples? What are the roles of space and spin dimensionalities in determining critical behavior? We hope to answer some of these questions in future work.

Another important matter to investigate is the extension of finite-size scaling to the specific heat in the Gaussian ensemble. We have been unable to do this at present mainly because of the numerical difficulties which arise as the system approaches the microcanonical ensemble. These are evident in Fig. 12 where large errors in $\langle C \rangle$

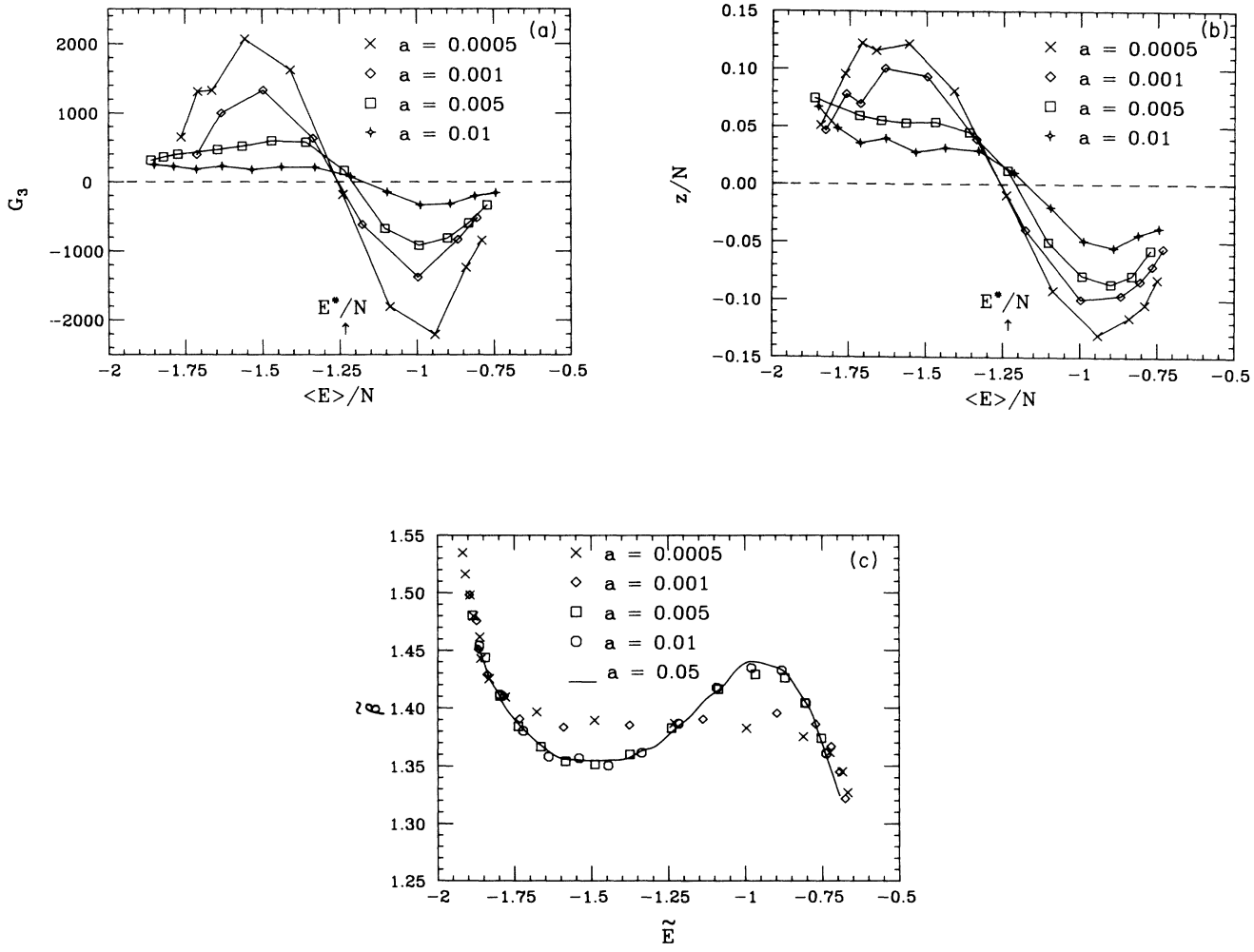

FIG. 7. (a) Behavior of $G_3 = \langle (E - \langle E \rangle)^3 \rangle$ at the first-order transition of Fig. 6(a), confirming that G_3 vanishes at E^*. The horizontal dashed line represents $G_3 = 0$ and the curves are straight-line interpolations between data points. G_3 data for $a = 0.005$ and 0.01 have been multiplied by 10 and 20, respectively, to enhance clarity. The fluctuations increase as the canonical ensemble is approached ($a \to 0$). G_3 also vanishes in the wings, $\beta = 0$ and ∞, where the energy distribution approaches a δ function. (b) Behavior of the third-order quantity z at the first-order transition of Fig. 6(a), confirming that it vanishes at E^*. z is obtained from Eq. (10) and represents the deviations of $\langle E \rangle$ and $\langle \beta \rangle$ from the microcanonical values. The horizontal dashed line represents $z = 0$ and the curves are straight-line interpolations between data points. z data for $a = 0.005$ and 0.01 have been multiplied by 3 and 5, respectively, to enhance clarity. (c) Scaled data at the first-order transition of Fig. 6(a), confirming that the values for large a collapse onto the microcanonical curve. $\tilde{E}$ and $\tilde{\beta}$ are estimates of the microcanonical values and are obtained through Eqs. (9a) and (12). The curve is from straight-line interpolations between data points for $a = 0.05$. Symbols have been omitted for $a = 0.05$ to maintain clarity.

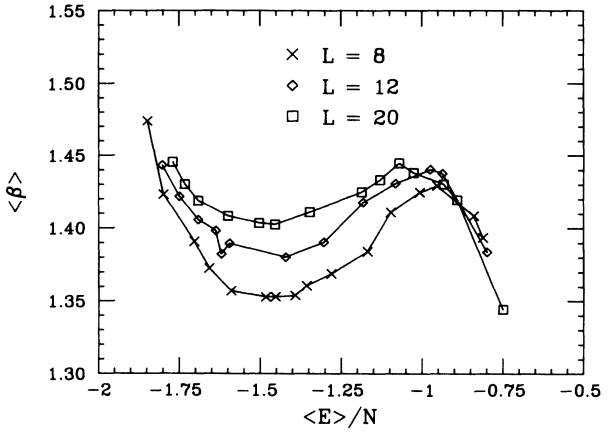

FIG. 8. Finite-N effects at the first-order transition of Fig. 6(a). N ($=L\times L$) is the number of particles and $aN=0.64$ was maintained for all data. Each data point represents averages over a minimum of 200 000 MCS. The curves are straight-line interpolations between data points. As N grows the loops approach the horizontal straight line which characterizes the energy discontinuity. Data for $L=10$ and 14 have been omitted for clarity.

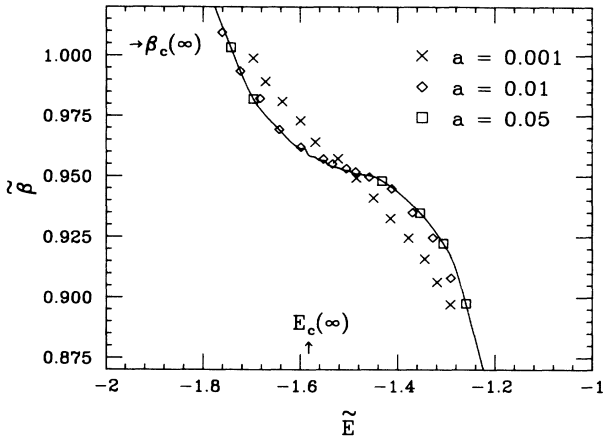

FIG. 10. Scaled $\langle\beta\rangle$-vs-$\langle E\rangle$ data at a second-order transition showing that the data collapse onto the microcanonical curve for large a. The data are for the $q=3$, $h=0$ model on an 8×8 lattice. Each data point in the transition region represents averages over 10^6 MCS. As in Fig. 7(c) there are significant deviations for small a. The curve is from straight-line interpolations between data points for $a=0.05$. (E^*,β^*) is the fixed point. $E_c(\infty)$ and $\beta_c(\infty)$ are infinite-lattice characteristics at the transition.

are present even after 10^6 MCS were used to compute the averages for only an 8×8 lattice.

IV. COMPUTATIONAL ADVANTAGES

The main advantage of the method lies in its ability to approach the microcanonical limit. Apart from making the diagnosis of the order of the transition easier, this also saves computer time at first-order transitions because, by using a sufficiently large value of a, we can directly sample the two-phase states. As shown in Ref. 17, this avoids the double-peaked distributions and the resulting hysteresis which are characteristic of canonical-ensemble simulations. Since the maxima of $P(E)$ grow with N, this feature becomes particularly attractive when large lattices are involved. For example, Fig. 14 shows the results for the $q=10$, $h=0$ model on a 50×50 lattice using $a=0.01$. We have deliberately limited the computing time to 5000 MCS per data point to emphasize the efficiency. The loop is clearly visible and we find that our estimates of $\beta_c(\infty)$, E_+, and E_- compare favorably with the exact values. Similar results us-

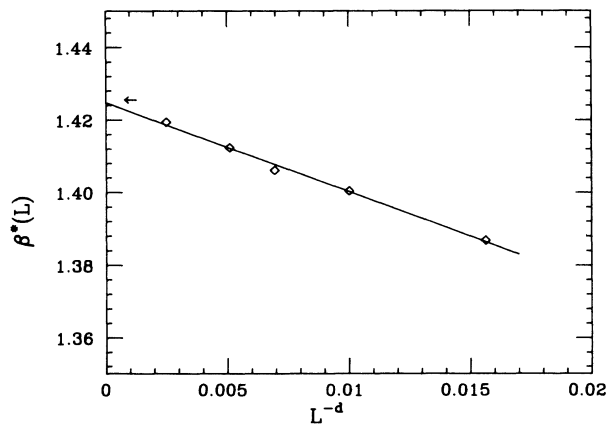

FIG. 9. Extrapolation of $\beta^*(L)$ vs L^{-d} to obtain $\beta_c(\infty)$ for the first-order transition of Fig. 6(a). For each L, $\beta^*(L)$ was defined as the fixed point as shown in Fig. 6(a). The straight line is the least-squares fit and yields $\beta_c(\infty)=1.4247$. The arrow denotes the exact result of $\beta_c(\infty)=1.426\,606\ldots$.

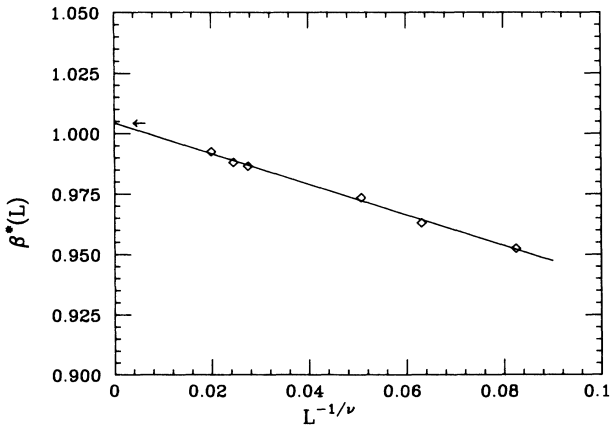

FIG. 11. Extrapolation of $\beta^*(L)$ vs $L^{-1/\nu}$ at the second-order transition of Fig. 10. den Nijs's conjectured value of $\frac{5}{6}$ was taken for the critical exponent ν (Ref. 29). $\beta^*(L)$ was obtained from the fixed points such as in Fig. 10 using $L=8$, 10, 12, 20, 22, and 26. The straight line is the least-squares fit and yields $\beta_c(\infty)=1.0043$. The arrows denotes the exact result of $1.005\,05\ldots$.

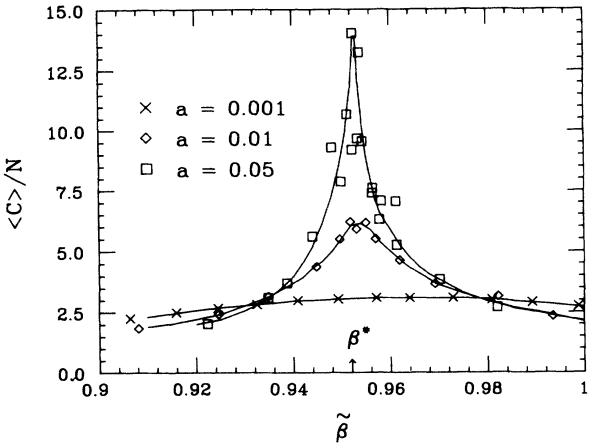

FIG. 12. Specific-heat data as a function of $\tilde{\beta}$ at the second-order transition of Fig. 10. The data for $L=8$ and various a are shown. The curves are smooth guides to the eye. The second-order transition is remarkably sharpened as one moves away from the canonical ensemble. See text for discussion.

ing the canonical ensemble on the same sample required over 10^6 MCS (Ref. 7). The problem there was that, due to the strong first-order transition, the 50×50 lattice in Ref. 7 spent as much as 5000 MCS in just one peak of $P(E)$ before flipping to the other.

While finite-N extrapolations are unavoidable for a conclusive diagnosis of the order of a transition, the fact that finite-N' effects are more prominent for small N in the Gaussian ensemble means that the method is very useful in the preliminary investigation of phase diagrams. As a first example we show in Fig. 15 results for the $d=3$, $q=3$, $h=0$ model which is believed to have a first-order transition. (See Ref. 29 for references to several approximate calculations for this model.) While Fig. 15 confirms this, the noteworthy point is that the entire computer run for producing the loop in this figure took up only 15 min on a fast scalar computer.

Figures 16 show the results for the $q=4$ and 5 models on 8×8 lattices. Figure 16(a) shows the data for the $q=5$, $h=0$ model and the first-order transition is evident. However, the size of the loop suggests a strong first-order transition, whereas the actual discontinuity is very small. This discrepancy is probably related to pathologies in the $q=5$ model, since extensive canonical-ensemble Monte Carlo simulations of the same model by other workers[31,32] using large lattices (up to $L=240$) and simulation times up to 10^6 MCS have revealed acute metastabilities[31] and extremely large correlation lengths.[32] We must emphasize that the method does not replace extrapolations to large N and what our calculation for the $q=5$, $h=0$ model shows is that for small N there is a wide region (in energy) in which $\ln[\rho(E)]$ is concave. The exact results for $E_+ - E_-$ indicate that this region narrows considerably as $N\to\infty$. We have found in the case of the $d=2$, $q=10$, $h>0$ model that what appears as a first-order transition for small N can disappear for larger N. Therefore, although the diagnosis is usually quite unambiguous for finite N, there is no way to avoid the process of extrapolation to $N\to\infty$. Figure 16(b) shows the results for the $q=5$ model in the presence of a large negative field. One of the states is thus suppressed [see Eq. (19) for a definition of the Hamiltonian] so that the $q=5$, $h=-\infty$ model is identical to the $q=4$, $h=0$ model which has a second-order transition. This indeed happens in Fig. 16(b) where the data for the $q=5$ model superimposes on the corresponding data for the $q=4$ model. We show this for two different values of a to demonstrate that the coincidence is not fortuitous.

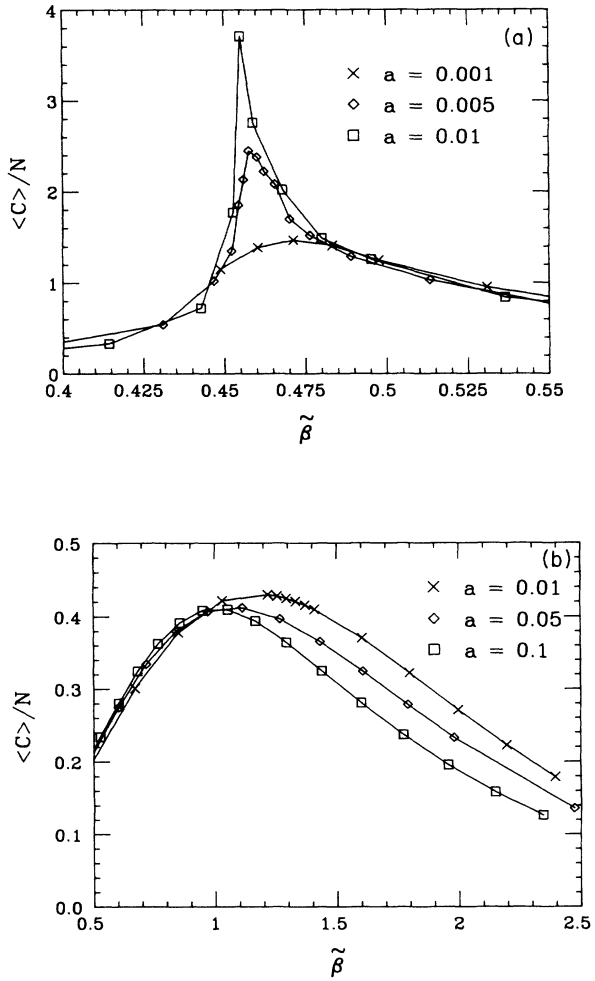

FIG. 13. (a) Specific-heat data for $N=4^3$ at the second-order transition in the $d=3$ Ising model in zero field. The behavior is similar to that in Fig. 12. The curves are straight-line interpolations between data points. Each data point represents averages over 100 000 MCS. (b) Specific-heat data for an $N=10$ Ising paramagnet, a noncritical model. There is no indication of the cusplike behavior characterizing Fig. 12 and (a). The spins $\{\sigma_i=\pm1\}$ in this model interact with a unit external magnetic field and the Hamiltonian is $H=-\sum_i \sigma_i$. The symbols are data from exact calculations since the density of states is known. The curves are straight-line interpolations between the data points.

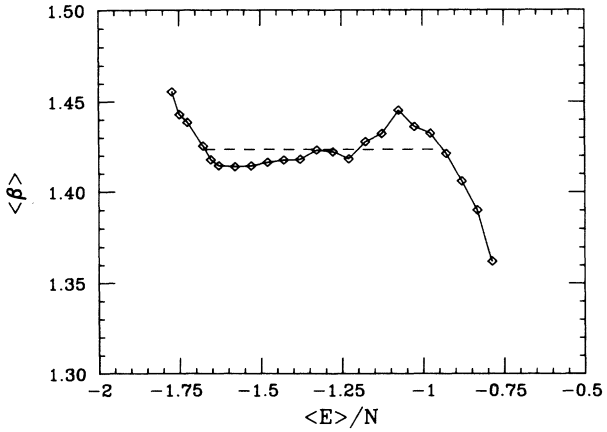

FIG. 14. Data for a large (50×50) lattice at the first-order transition of Fig. 6(a) using $aN=0.01$. The curve consists of straight-line interpolations between data points which are averages over 5000 MCS each. The horizontal dashed line is the equal-area construction and yields $E_-=-1.672$, $E_+=-0.938$, and $\beta_c=1.424$. The exact results are -1.663, -0.9682, and 1.4261, respectively.

V. SUMMARY AND FUTURE WORK

We have shown that the Gaussian ensemble is intermediate to the canonical and microcanonical ensembles which are the limiting cases of this method. $Q_a(E_t)$, the analog of the partition function, defined through Eq. (4) and the fluctuation formula for the specific heat, Eq. (3), show this analytically, while the interpretation of the temperature in Fig. 3 provides a graphic demonstration of this interpolating property. The stability criterion (8) shows that, by reducing the size of the bath, states with negative specific heat can be sampled at first-order transitions leading to van der Waals loops in $\beta(E)$. This feature has proven useful in distinguishing the first- and second-order transitions in Potts models in both $d=2$ and 3. In particular, we have shown in Sec. IV that the method confirmed easily that $q_c=4$ and 2 for $d=2$ and 3, respectively. Note that these are significant results; for example, the canonical-ensemble simulations of Binder[33] could not distinguish the weak first-order transition in the $d=2$, $h=0$, $q=5$ model even after a relatively substantial computational effort. It would be interesting to see whether the method is equally successful in diagnosing the order of the transition in more complicated mod-

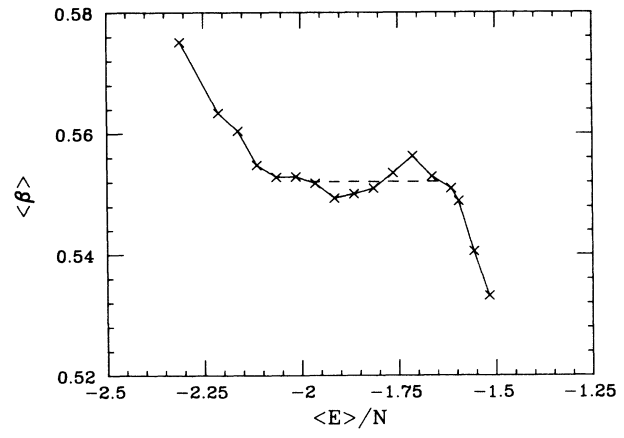

FIG. 15. $\langle\beta\rangle$-vs-$\langle E\rangle/N$ curves for the $d=3$, $q=3$, $h=0$ model. Data are for $N=4^3$ and $a=0.05$. Each point represents averages over 50 000 MCS and the curves are straight-line extrapolations between data points. The dashed line is the equal-area construction. The loop confirms the first-order transition diagnosed by other workers.

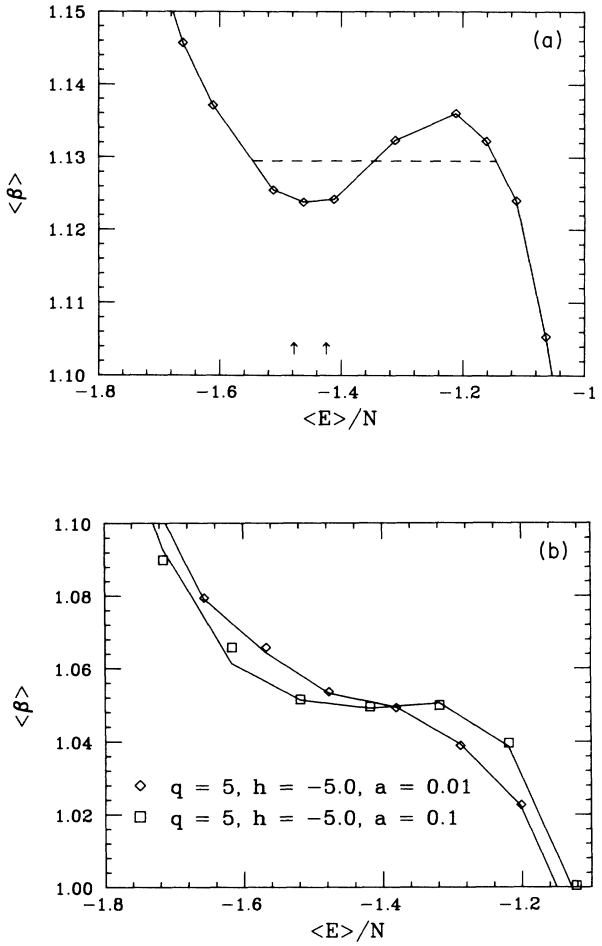

FIG. 16. (a) Results at the first-order transition in the $d=2$, $q=5$, $h=0$ model on an 8×8 lattice using $a=0.1$. The dashed line is the equal-area construction. The arrows indicate the location of E_- and E_+, the infinite-lattice energies at the transition. The exact value of $\beta_c(\infty)$ is 1.174 359... and lies outside the scale of the figure. The size of the discontinuity, E_+-E_-, as suggested by the data for $L=8$ is an order of magnitude larger than the true value. (b) Equivalence of the $q=5$, $h\ll 0$ model and the $q=4$, $h=0$ model in $d=2$. The data are for an 8×8 lattice using two different values of a and 500 000 MCS per data point in the transition region. The curves are for the $q=4$ model and are straight-line interpolation between data points. Symbols for $q=4$ have been omitted to preserve clarity.

els such as frustrated Ising models on cubic lattices.[34]

The simple expression for the entropy of the bath facilitated the analysis of the N'-dependent effects in the $\langle\beta\rangle$-versus-$\langle E\rangle$ curves and is an advantage over Creutz's method.[12] By means of theorem 3 we have shown the fundamental nature of the microcanonical curve, $\tilde{\beta}(\tilde{E})$, for finite samples and have verified this through the curves in Fig. 6(a). The leading-order deviations from $\tilde{\beta}(\tilde{E})$ for $N'>0$ have been shown to be due to third-order terms in the energy fluctuations and the correctness of the analysis was demonstrated by obtaining the microcanonical curves in Figs. 7(c) and 10. The vanishing of the third-order quantity G_3 irrespective of N' at the inflection point in $\tilde{\beta}(\tilde{E})$ at a phase transition provided a novel definition for the transition temperature $\beta^*(N)$ in finite samples. We have shown that $\beta^*(N)$ extrapolated correctly to the exact value of $\beta_c(\infty)$ at the first-order transition in the $d=2$, $q=10$ model and also the second-order transition in the $d=2$, $q=3$ model. The latter also confirmed den Nijs's conjectured value[29] of $\frac{5}{6}$ for the critical exponent ν in the $d=2$, $q=3$ model.

It is straightforward to apply the Gaussian ensemble to obtain intensive quantities other than the temperature. Thus, by using an ensemble where β and the total magnetization of the bath and sample are constants, Stump[16] could obtain the magnetic field h using the definition $\partial S/\partial m=-h/\beta$ where m is the magnetization of the sample. Similarly, keeping β and the total volume of the bath and sample constant, one can deduce the pressure p through $\partial S/\partial v=\beta p$, where v is the volume of the sample. In Appendix B we show a novel way to apply the idea of a finite bath with known entropy to the simulation of classical systems of the type investigated in molecular dynamics but without actually doing the dynamical calculations.

There are some points about the method which remain to be clarified. At first-order transitions, it would be instructive to analyze the loops along the lines of Mayer and Wood[35] and extract information on the surface tension. This should prove useful in applying the method to the study of nucleation phenomena[36] and melting of microclusters.[37] As regards second-order transitions, we need to explain the sharpening of the specific-heat peaks for large a. Finally, whether the cusps are present or not, it is necessary to extend finite-size scaling to incorporate the N'-dependent effects.

ACKNOWLEDGMENTS

We thank Professor S. D. Mahanti, Professor T. A. Kaplan, Professor K. Kubo, Professor D. R. Stump, and Professor M. E. Fisher for several useful comments during the course of this work and Professor R. S. Berry and Dr. G. S. Grest for copies of their work prior to publication.

APPENDIX A

We demonstrate here how to choose the parameters E_t and (especially) the value of a which would yield the effective microcanonical curve. Note that a and E_t specify a linear relation between β and $\langle E\rangle$ through the equation

$$\beta=2a(E-E_t)\ , \tag{A1}$$

and the calculation determines the location of β and E on this line.

Choice of a. If nothing is known about the sample's thermodynamics, the following criterion may be used. Let ΔE be the typical allowed change in the sample's energy in one "spin flip." Then a may be chosen as

$$a=(\Delta E)^2/N\ .$$

Once the approximate form of the β-versus-E curve is known, it is possible to experiment with a. This is best done by plotting the linear equation for β above on top of the $\beta(E)$ curve and adjust a, remembering that if $\beta(E)$ intersects the straight line more than once, there is a double-peaked probability distribution with its attendant metastability. Therefore a should be kept large enough so that the line has a greater slope than the largest positive value of $d\beta/dE$.

Choice of E_t. Once a is chosen, E_t can be swept through a range of values producing the β-versus-E curve. Keeping in mind that we are referring always to negative energies, E_t will always be less than E and can be adjusted to cover the range of β and E desired. As more information is obtained about the $\beta(E)$ curve, Eq. (A1) may be used in reverse to determine the range of E_t required to produce data for a different value of a.

APPENDIX B

Simulation of classical systems is possible by treating the kinetic energy K as a heat bath connected to the potential energy V through the equation $E=K+V$. The thermodynamics of the kinetic energy can be done analytically and we find that the density of states of the "bath" is given by

$$\int_0^K \rho(K)dK=\Omega(\sqrt{2mK})\ ,$$

where $\Omega(r)$ is the volume of a $3N$-dimensional sphere of radius r. Therefore

$$\rho(K)=\frac{d\Omega}{dK}=BK^{(3N-2)/2}\ ,$$

where B is (for us) an uninteresting geometric constant. Therefore we propose to do the Monte Carlo procedure on $V(r)$, calculating the probability of a step being accepted on the basis of the ratio

$$R=\left[\frac{E-V(r')}{E-V(r)}\right]^{(3N-2)/2}$$

instead of the more familiar $e^{-\beta(E'-E)}$. Temperature is given in the same way as is usual for microcanonical calculations:

$$\beta=\frac{1}{\rho(K)}\frac{\partial\rho(K)}{\partial K}=\frac{(3N-2)}{2(E-\langle V\rangle)}\ .$$

Thus if we want only thermodynamic information about an isolated classical system, it is not necessary to implement Newton's equations of motion—the whole process can be carried out by sampling the potential energy itself.

[1]N. Metropolis, A. W. Rosenbluth, M. N. Rosenbluth, A. H. Teller, and E. Teller, J. Chem. Phys. **21**, 1087 (1953).

[2]*Monte Carlo Methods in Statistical Physics,* edited by K. Binder (Springer-Verlag, New York, 1979).

[3]B. J. Alder and T. E. Wainwright, J. Chem. Phys. **27**, 120 (1957).

[4]A. Rahman, Phys. Rev. **136**, A405 (1964).

[5]B. J. Alder and T. E. Wainwright, Phys. Rev. **127**, 359 (1962). The loops in this work and some other references to follow were actually in the pressure-volume isotherms of a fluid. The discussion remains the same, however, if we substitute "compressibility" for "specific heat."

[6]C. L. Briant and J. J. Burton, J. Chem. Phys. **63**, 2045 (1975).

[7]M. S. S. Challa, D. P. Landau, and K. Binder, Phys. Rev. B **34**, 1841 (1986).

[8]W. W. Wood, in *Physics of Simple Liquids,* edited by H. N. V. Temperley, J. S. Rowlinson, and G. S. Rushbrooke (North-Holland, Amsterdam, 1968), pp. 176–182. See also p. 143. Wood notes that the loops of Ref. 5 could not be reproduced by canonical-ensemble Monte Carlo methods.

[9]A recent review of finite-size scaling at second-order transitions is given by M. N. Barber, in *Phase Transitions and Critical Phenomena,* edited by C. Domb and J. L. Lebowitz (Academic, New York, 1983), Vol. 8, p. 145.

[10]Finite-size effects at first-order transitions have been dealt with by a number of workers. See, for example, Y. Imry, Phys. Rev. B **21**, 2042 (1980); M. E. Fisher and A. N. Berker, *ibid.* **26**, 2507 (1982); J. L. Cardy and M. P. Nightingale, *ibid.* **27**, 4256 (1983); V. Privman and M. E. Fisher, J. Stat. Phys. **33**, 385 (1983); K. Binder and D. P. Landau, Phys. Rev. B **30**, 1477 (1984).

[11]J. Jellinek, T. L. Beck, and R. S. Berry, J. Chem. Phys. **84**, 2783 (1986).

[12]M. Creutz, Phys. Rev. Lett. **50**, 1411 (1983).

[13]J. H. Hetherington, J. Low Temp. Phys. **66**, 145 (1987).

[14]J. H. Hetherington and D. R. Stump, Phys. Rev. D **35**, 1972 (1987).

[15]D. R. Stump and J. H. Hetherington, Phys. Lett. B **188**, 359 (1987).

[16]D. R. Stump, Phys. Rev. A **36**, 365 (1987).

[17]M. S. S. Challa and J. H. Hetherington, Phys. Rev. Lett. **60**, 77 (1988).

[18]F. Reif, *Fundamentals of Statistical and Thermal Physics* (McGraw-Hill, New York, 1965).

[19]C. Kittel, *Thermal Physics* (Wiley, New York, 1969).

[20]R. K. Pathria, *Statistical Mechanics* (Pergamon, New York, 1972).

[21]J. Hansen and L. Verlet, Phys. Rev. **184**, 151 (1969).

[22]M. A. A. da Silva, A. Caliri, and B. J. Mokross, Phys. Rev. Lett. **58**, 2212 (1987).

[23]W. W. Wood, in Ref. 8, pp. 156 and 157.

[24]R. K. Pathria, in Ref. 20, pp. 69–74.

[25]R. K. Pathria, in Ref. 20, pp. 376 and 377.

[26]For a review of Potts models, see F. Y. Wu, Rev. Mod. Phys. **54**, 235 (1982).

[27]R. J. Baxter, J. Phys. C **6**, L445 (1973).

[28]T. Kihara, Y. Midzuno, and T. Shizume, J. Phys. Soc. Jpn. **9**, 681 (1954).

[29]This conjecture is believed to be true. See M. P. M. den Nijs, J. Phys. A **12**, 1857 (1979) for details.

[30]C. N. Yang and T. D. Lee, Phys. Rev. **87**, 404 (1952); **87**, 410 (1952).

[31]E. Katznelson and P. G. Lauwers, Phys. Lett. B **186**, 385 (1987).

[32]P. Peczak and D. P. Landau, Bull. Am. Phys. Soc. **33**, 584 (1988).

[33]K. Binder, J. Stat. Phys. **24**, 69 (1981).

[34]G. S. Grest, J. Phys. C **18**, 6239 (1985), and references therein. Grest notes that canonical-ensemble Monte Carlo methods could not conclusively identify the first-order transition in the fully frustrated models.

[35]J. E. Mayer and W. W. Wood, J. Chem. Phys. **42**, 4268 (1965).

[36]For a review of nucleation phenomena, see J. D. Gunton, in *Phase Transitions and Critical Phenomena,* edited by C. Domb and J. L. Lebowitz (Academic, New York, 1983), Vol. 8.

[37]G. Natanson, F. Amar, and R. S. Berry, J. Chem. Phys. **78**, 399 (1983).